Solid-state NMR studies of weak interactions in supramolecular systems

Michele R. Chierotti and Roberto Gobetto*

Received (in Cambridge, UK) 30th July 2007, Accepted 28th November 2007
First published as an Advance Article on the web 7th January 2008
DOI: 10.1039/b711551b

The field of application of solid-state NMR to the study of supramolecular systems is growing rapidly, with many research groups involved in the development of techniques for the study of crystalline and amorphous phases. This Feature Article aims to provide an overview of the recent contributions of our research group to this field, paying particular attention to the study of the weak interactions such as hydrogen bonds in supramolecular systems through solid-state NMR investigations. The structure and dynamic behaviour of selected host–guest systems will be also discussed.

Introduction

Supramolecular chemistry, based on non-covalent interactions is becoming increasingly important relative to conventional molecular chemistry based on covalent bonds. It is a rapidly expanding discipline devoted to the design, by means of weak interactions (electrostatic forces, hydrogen bonds, van der Waals interactions, ...), of periodic and organized supramolecular structures with desired properties.[1] Nowadays, supramolecular chemistry represents a major branch of science, involving interdisciplinary chemical, physical, biological and technological aspects of the creation and study of complex supramolecular systems. Furthermore, it covers many research areas such as the macrocyclic chemistry and its applications,[2] nanochemistry,[3] supramolecular catalysis,[4] self-assembly processes[5] and dendrimers.[6]

The common feature of the research in all of these fields is the stored information in the molecular and supramolecular structures. In all of these areas weak interactions play the most important role on the basis of their highly specific functions in biological systems, such as molecular recognition, transport, catalysis, regulation, *etc.*, as well as in crystal engineering (CE), and in mechanical properties of materials.

Our interest, centred on weak interactions (mainly hydrogen bonds and van der Waals contacts) is twofold: first it is oriented towards the study of the hydrogen bond (HB) as a tool for molecular self-assembly in the field of the CE. In addition we would like to investigate how these weak interactions affect the mobility of molecules in model samples such as the inclusion complexes.

A central aspect of CE concerns the construction of crystalline materials from discrete molecular building blocks using non-covalent interactions.[7] Indeed, in the supramolecular approach to crystalline solids the crystals are seen as networks of weak contacts. Though these supramolecular connections are weaker than covalent bonds, they are able to cooperatively assemble molecules thanks to the large number of directional interactions. The rational design of crystal structures depends heavily on the understanding and exploitation of such intermolecular forces and on the predictability of molecular self-organization.[8] Among the different spectroscopic techniques available for the study of the supramolecular systems, high-resolution solid-state NMR often represents the technique of choice if the goal is the careful inspection of the specific site of the intermolecular interaction. It is well known in fact that solid-state NMR is able to investigate the microscopic environment at each individual site in a solid material and has therefore emerged as a powerful technique especially in solid systems lacking the order or homogeneity for crystallographic

Università degli Studi di Torino, Dipartimento di Chimica I.F.M, Via P. Giuria 7, 10125 Torino, Italy. E-mail: roberto.gobetto@unito.it; Fax: +39 0116707855; Tel: +39 0116707523

Michele R. Chierotti

Michele R. Chierotti graduated from the University of Torino in 2002 with a thesis researched at the IVIC (Caracas, Venezuela). In 2006 he received a PhD degree in Chemical Science. He spent a period at the university of Durham (UK) with Prof. Robin K. Harris. From 2006 he took a postdoctoral position at the University of Torino.

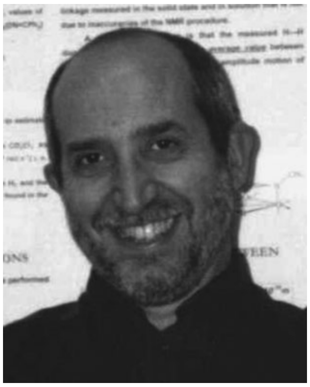

Roberto Gobetto

Roberto Gobetto was born near Torino (Italy) in 1956. Researcher since 1983 at the University of Torino he is currently professor of Inorganic Chemistry. He has served as visiting professor at the University of Northridge (USA) and at University of Durham (G.B.). His main research interests focus on organometallic chemistry, luminescent probes, hyperpolarization and solid-state NMR.

examinations.[9] In principle not only the microscopic environment affects the chemical shift of the nuclei involved in the interaction, but also a wealth of other local parameters (quadrupolar and dipolar interactions, chemical shift anisotropy (CSA), *etc*, …), directly reports on the geometric and electronic structure for the complete characterization of the material. An other important point to consider is the general increase in the possibility of dynamic behaviour for single groups or entire molecules in the solid state when weak non-covalent interatomic forces are present. This is typical, for example, of host–guest adducts, where lower activation energy barriers are expected for the motion of molecules within the cavity or the channel of a matrix. The mobility in a solid-state inclusion environment represents a different dynamic regime in comparison with both solution and crystalline situations.

Single-crystal X-ray structures of host–guest complexes with simple neutral guest molecules are often difficult to obtain and therefore solid-state NMR methods[10] have been heavily used for the elucidation of such inclusion compounds.

The importance of solid-state NMR techniques for the study of dynamics is due primarily to its ability to detect correlation times of motion in the range 10^{-1} to 10^{-10} s.[11] Different solid-state NMR experiments in low resolution (wideline) and high resolution (lineshape analysis at variable temperature, CSA analysis, 2D-EXSY, relaxation time studies, *etc*.) can be customized for detecting and quantifying molecular motions involving individual groups or entire molecules.

In this paper we would like to present some of our recent solid-state NMR studies on supramolecular systems. Special emphasis will be focused on the different NMR parameters available to a spectroscopist for the complete understanding of the interplay of intermolecular interactions with the structure and dynamics of molecules in supramolecular systems. Then, several examples of guest motion in host–guest systems formed between cyclodextrin (CD) and organometallic compounds will be presented. The extent of guest dynamics is shown to be dependent on the degree of symmetry of the guest complex and the interaction with the CD cavity.

Investigation of hydrogen bond

HB plays a fundamental role in CE[12] due to its directionality, specificity, strength and selectivity.[13] In addition the characteristic qualities of transferability (from crystal to crystal), reproducibility (in terms of cohesive contribution to crystal packing) and ease of chemical manipulation (molecular functionalisation with hydrogen-bonding donor/acceptor systems) make it the most used cement in CE synthesis. For these reasons there has been an increasing number of papers devoted to the self-organization of organic molecules into one-, two- or three-dimensional hydrogen-bonded architectures.[12–14]

Their strengths can vary from 5 kJ $\mathrm{mol^{-1}}$ to hundreds of kJ $\mathrm{mol^{-1}}$ depending on the molecules and whether they are in the gas phase or in solution.[15] The enthalpies of weak HBs involving oxygen and nitrogen are in the range 16–40 kJ $\mathrm{mol^{-1}}$,[16] but it has been reported for low-barrier hydrogen bonds, LBHBs, that the strength can be as high as 50–100 kJ $\mathrm{mol^{-1}}$.[17]

The energy of weak HBs is usually dominated by electrostatic factors while strong ones are short in length and show magnetic and vibrational properties that are consistent with a covalent rather than electrostatic attraction (Fig. 1). However, we cannot ignore polarization, charge transfer and exchange repulsion that also play important roles.

HBs have been divided, based on their strength, into three categories, namely strong, moderate, and weak. In weak HBs the heavy atoms are separated by less than the sum of their van der Waals radii *i.e.* for $\mathrm{O\cdots H\cdots O} \leq 2.6$ Å, for $\mathrm{N\cdots H\cdots N} \leq 2.8$ Å and for $\mathrm{N\cdots H\cdots O} \leq 2.7$ Å, while in strong HBs the heavy-atom distances are 2.4–2.55 Å for $\mathrm{O\cdots H\cdots O}$, 2.6–2.7 Å for $\mathrm{N\cdots H\cdots N}$ and 2.5–2.6 Å for $\mathrm{N\cdots H\cdots O}$.[17]

Due to their importance not only in CE but also in many others fields and due to the difficulties in detecting and characterising them, several techniques have been used for the detection and characterization. Neutron diffraction crystallography is certainly the most definitive way, but low-temperature X-ray crystallography can also be used.[18]

However, these techniques have some intrinsic limitations and cannot be universally applied. This is, for example, the case for products obtained by means of solvent-free methods such as those occurring in the solid state between molecules (solid–solid) or between a solid and a gas. For instance, mechanical processing based on co-grinding or milling of solids which is a scalable technique routinely used in materials science,[19] in the pharmaceutical industry,[20] for the synthesis of novel molecular compounds,[21] and, recently, has also been utilized in the field of CE.[22] The basic idea is that of breaking and forming supramolecular interactions with no need for the intermediacy of a solvent. However, these powdered products do not permit a straightforward determination of the structural features, of the type obtainable from single crystals. The problem can sometimes be circumvented by growing crystals of the desired phase *via* seeding, *i.e.* by using preformed microcrystals, in the form of crystalline powder, obtained by grinding.[23] If single crystals are obtained *via* seeding, it is possible to verify a posteriori whether the material obtained from solution crystallization and that yielded by solid–solid processes possess the same structure, by comparing the observed powder diffraction pattern with that computed on the basis of the single-crystal structure (Fig. 2). However when this kind of analysis is not possible the alternative investigation techniques are mainly IR and solid-state NMR spectroscopies.

IR and NMR spectroscopies have both become standard methods for investigating HBs in the solid state.[24] Comparing solution and solid-state NMR the latter allows a more accurate study since the signals are not averaged by solvent effects or by rapid exchange processes often present in solution.

Concerning supramolecular adducts, a large interest is growing in the features of the formed species, *i.e.* whether they are neutral (co-crystal) or ionic (salts) and thus to ascertain if a proton transfer reaction from the acid to the base along the HB takes place or not. Of particular interest in this regard are solid-state NMR experiments that investigate either the hydrogen atom directly involved in the HB (employing ^{1}H or ^{2}H NMR techniques) or the atoms within, or in close proximity to the HB donor and acceptor groups (employing ^{13}C, ^{15}N, ^{17}O, ^{29}Si or ^{31}P NMR techniques).[25] The versatility

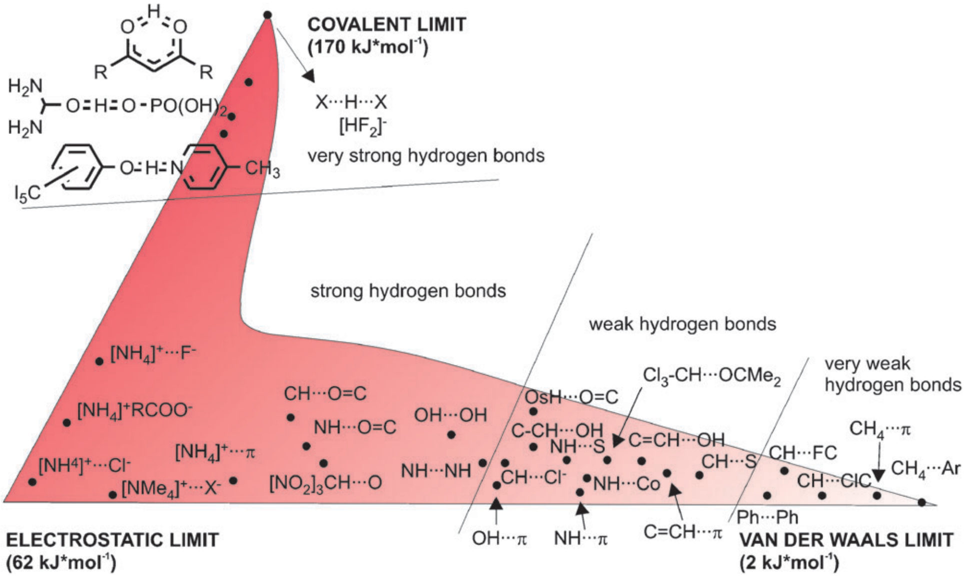

Fig. 1 Schematic and non-quantitative representation of interactions dominating the energy of hydrogen bonds. Reproduced with permission from ref. 14*c*. Copyright 2002, American Chemical Society.

of solid-state NMR arising from its multinuclear capability is highlighted.[26] In addition, the dependence of NMR measured parameters (mainly the chemical shifts, the CSA, the dipolar and quadrupole coupling constants, *etc.*) on the strength and geometry of hydrogen bonding has been discussed in detail.[17,27]

Here we briefly present the main parameters that can provide insights on the HB interactions in the solid state: (a) chemical shift, (b) double quantum transitions, (c) chemical shift anisotropy (CSA), (d) relaxation parameters, (e) isotopic effect.

Chemical shift

One of the important aspects of solid-state NMR is the multinuclei approach. Indeed, in most HBs several nuclei may be observed by NMR spectroscopy.

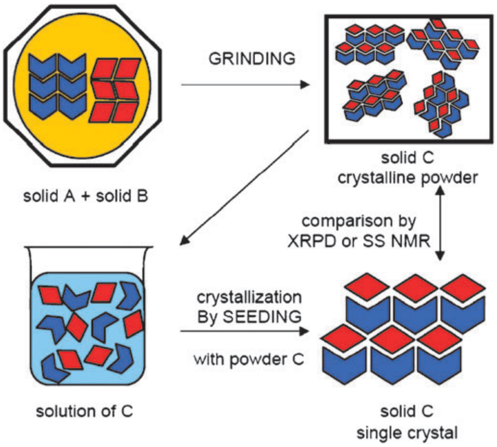

Fig. 2 Representation of the procedure for characterizing products obtained by means of solid-solid processes. Reproduced with permission from ref. 23*b*. Copyright 2004, Wiley-VCH Verlag GmgH & Co. KGaA.

^{1}H Chemical shift

The development of line narrowing techniques in solids *i.e.* the possibility of spinning the sample (MAS) at speeds higher than 20 kHz allows the location of chemical shifts of hydrogen-bonded protons leading to an increasing number of ^{1}H studies.[28] In particular, the proton is increasingly deshielded with increasing the HB strength, which leads to ^{1}H high-frequency shifts far from the aliphatic and aromatic signals (Scheme 1). The main feature of this technique is that the magnitude of the shift is directly correlated with the length of the HB.[24,29] Frey[17] and Sternberg[30] have observed direct relationships between $\delta(^1H)$ and HB strength and between $\delta(^1H)$ and X–H distance for different classes of hydrogen-bonded compounds. In a series of previous reports this relationship in solid peptides has been theoretically and experimentally elucidated.[31] Correlation between the $\delta(^1H)$ and the heteroatom separation supports this interpretation (Fig. 3).[32] In the case of O···H···O contact, Th. Emmler *et al.*,[33] have proposed a correlation between the ^{1}H chemical shift of hydrogen-bonded protons and the HB geometry of neutron crystallography structures.

Thus, NMR shift data can be used to detect and to estimate the presence and the strength of HBs (Fig. 5).

Since the HB can be seen as an incipient proton transfer reaction, many studies have been done by probing, through

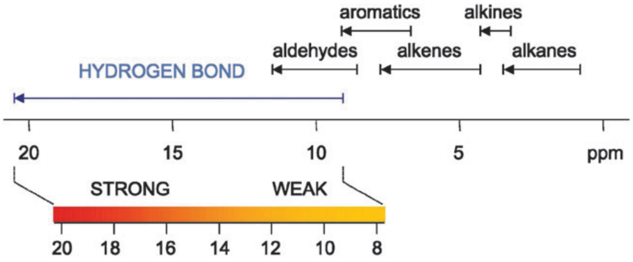

Scheme 1 ^{1}H NMR chemical shift scale.

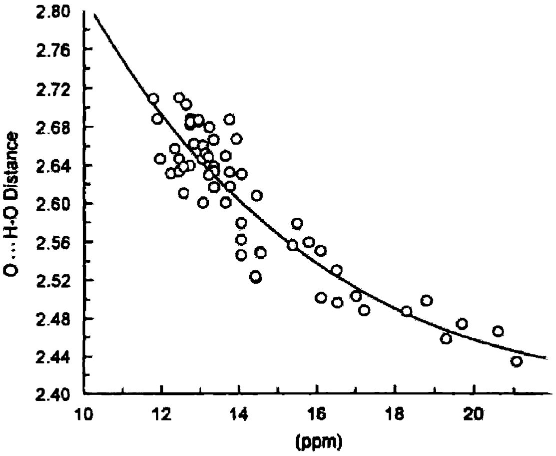

Fig. 3 Correlation between O···H–O distance and ^{1}H chemical shift. The curve provides a method for calculating the hydrogen bond length in crystalline amino acid by NMR. Reproduced with permission from ref. 32*a*. Copyright 2000, Elsevier.

the proton chemical shift, the H position and the HB strength as a function of the pK_a or the pK_b of the acid or base moieties or as a function of the temperature.[28,33,34] For instance, the proton transfer reaction in supramolecular adducts between aliphatic dicarboxylic acids and the diamine 1,4-diazabicyclo[2.2.2]octane (DABCO) has been probed by varying the acid chain length (Fig. 4).[35] The ^{1}H MAS NMR study (Fig. 5) has shown that intramolecular O–H···O and intermolecular N···H–O HBs are strong interactions, with proton chemical shifts of around 16 ± 1.5 ppm, and N···O and O···O bond lengths of around 2.55–2.60 Å, while intermolecular $^+$N–H···O$^-$ interactions are weaker and are characterised by a δ(^{1}H) of about 12.3 ppm and by an N···O bond length of about 2.7 Å.[36]

In the case of the two forms of the cincomeronic acid data resulting from ^{1}H MAS NMR, combined with IR and Raman spectra, have explained the thermodynamic relationship between the two polymorphs confirming the presence of strong N–H···O interactions in form I while in form II they are significantly weaker.[37]

Due to the intrinsic difficulty of the X-ray technique in detecting the hydrogen atom position, an effective method that combines ^{1}H MAS NMR and DFT calculations for the determination of the HB O–H distance has been proposed (Fig. 6).[36,38] It has been shown that using the experimental ^{1}H chemical shift in the plot of the calculated chemical shifts *vs.* bond lengths is useful for obtaining a good estimation of the hydrogen atom positions. The method has been validated by comparing the N–H distance in HBs of methylnitroacetanilide obtained by different techniques such as neutron diffraction, X-ray diffraction and NMR dipolar coupling.[38]

^{1}H Double quantum (DQ) transitions

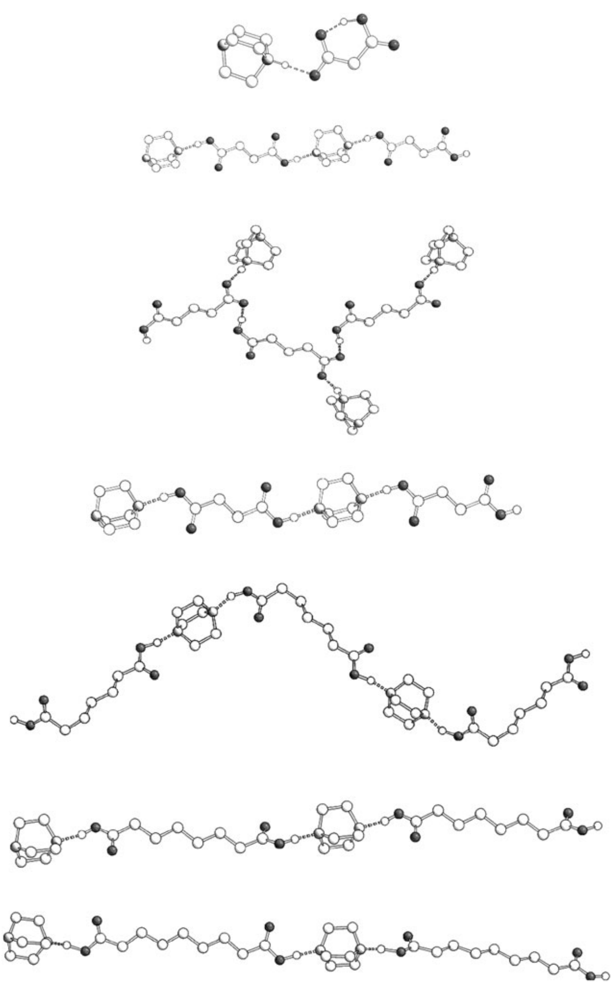

Fig. 4 Crystal structure of supramolecular adducts between DABCO and dicarboxylic acids with variable chain length of formula HOOC(CH$_2$)$_n$COOH with n = 1–7. Reproduced with permission from ref. 36. Copyright 2005, American Chemical Society.

If the development of high-speed (rotor speed ω_R >25 kHz) magic angle spinning probes allows improved resolution by averaging the homonuclear dipolar coupling,[39] by means of multidimensional NMR experiments it is possible to obtain additional information unavailable from one-dimensional (1D) spectra even in the limit of high resolution. The combination of fast MAS with 2D multiple quantum (MQ) spectroscopy have been successfully employed in the structural and

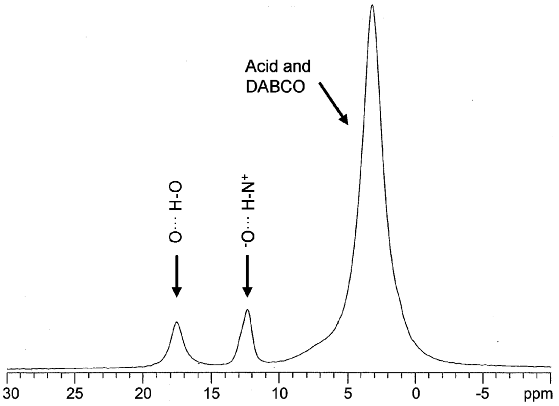

Fig. 5 ^{1}H MAS NMR spectrum of DABCO–malonic acid adduct recorded at 500 MHz with a spinning speed of 30 kHz. Reproduced with permission from ref. 36. Copyright 2005, American Chemical Society.

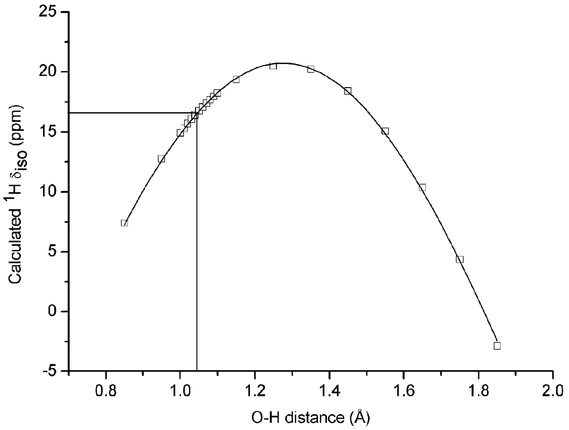

Fig. 6 Plot of the calculated ^{1}H chemical shift *vs.* the O–H distance. By using the experimental ^{1}H chemical shift obtained from the ^{1}H MAS spectrum for fitting the curve it is possible to obtain a reliable O–H distance for the hydrogen bond under investigation. Reproduced with permission from ref. 36. Copyright 2005, American Chemical Society.

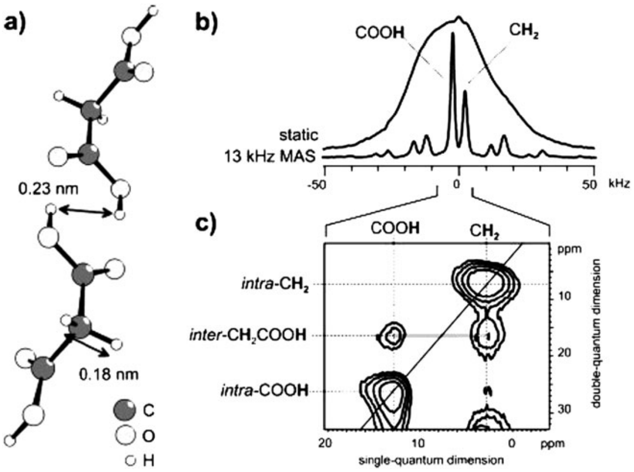

Fig. 7 (a) Carboxylic acid groups arrangement in the crystal packing of the malonic acid with interproton distances obtained from ^{1}H SQ and DQ MAS spectra. (b) 1D ^{1}H static and MAS (13 kHz) spectra of malonic acid. (c) ^{1}H DQ MAS spectrum of malonic acid recorded at 13 kHz at a ^{1}H Larmor frequency of 500 MHz. Reproduced with permission from ref. 45. Copyright 2001, Elsevier.

dynamic investigations of hydrogen bonded,[40] dendritic,[41] liquid crystalline,[42] and polymeric materials.[43] In rigid systems, the one-dimensional ^{1}H MAS spectrum gives chemical information *via* the chemical shift while the analysis of rotor encoded ^{1}H DQ MAS spinning sideband patterns enables the quantitative determination of the internuclear distance for a well-isolated pair of protons.[44] In mobile systems, the ^{1}H–^{1}H dipolar interaction is averaged and the magnitude of the extracted coupling constant from the DQ spectrum can yield characteristic information regarding the motional averaging process.[42,43] The simplicity of this technique which, for example, requires neither isotopic labeling nor crystalline materials, makes it an attractive new tool for studying the arrangement and packing of the key building blocks of systems generated in the rapidly developing field of supramolecular chemistry.

Schnell and Spiess have exhaustively reviewed the HBs present in carboxylic acid dimers and also in more extended hydrogen-bonded arrays used for the formation of supramolecular polymers by linking bifunctional monomers.[45]

Fig. 7 shows, for example, the information available from 1D and 2D ^{1}H DQ MAS spectra in the case of malonic acid. Each signal can be unequivocally assigned to each proton, and the chemical shift of the carboxylic protons can be correlated with the O···O distance. Furthermore the intermolecular correlation between CH$_2$ and COOH protons can be used as a parameter for establishing the conformation and array structure in the solid state.[45]

Since the DQ signal pattern directly reflects the spatial proximities between the different proton species involved, different arrays of multiple HBs of two tautomeric forms of the dimer ureido–pyrimidinone have been directly identified in the solid state. These units were used as a model for recognizing the two corresponding supramolecular polymers.[46]

In another paper, with the aid of 2D ^{1}H DQ MAS spectra Diez-Peña *et al.* were able to distinguish three types of proton (peaks at 8, 10.5 and 12.5 ppm) in collapsed poly(methacrylic acid): one belonging to carboxylic acid (8 ppm) and two arising from different types of hydrogen-bonded forms (10.5 and 12.5 ppm). Furthermore, the stability of the these HBs has been deduced from the H···H distances within the dimers, obtained from the analysis of the DQ MAS sideband patterns.[47]

In addition, attention has focused on the development of methods suitable for the measurements of heteronuclear dipolar couplings between protons and other spin I ($I = 1/2$) nuclei (*i.e.*, ^{1}H–^{13}C and ^{1}H–^{15}N).[48]

^{15}N Chemical shift

The ^{15}N chemical shift is also a useful parameter for the location of the hydrogen in HB systems involving nitrogen and oxygen atoms. It is expected that the ^{15}N chemical shift is more sensitive to the presence of the HB than that of other nuclei such as ^{1}H and ^{13}C, due to the wider chemical shift range of the former. For example, aliphatic amines involved in HBs show in solution high-frequency shifts of 1–5 ppm when interacting with donor solvents, whereas the high-frequency shift is of the order of 10–25 ppm in the case of protonating solvents.[49]

Because solid-state signals are not averaged by solvent effects or by rapid exchange processes present in solution, the change in the nitrogen chemical shifts caused by complete protonation can be of the order of 50–100 ppm, allowing a more accurate study.[50]

Intermolecular HBs produce a high- or low-frequency shifts in the ^{15}N values, according to the type of nitrogen atom and to the type of interaction (Scheme 2).[51]

For the ^{15}N isotropic chemical shift the protonation-induced shifts are of the order of 100 ppm towards lower frequencies for aromatic amines, and of about 25 ppm towards higher frequencies for aliphatic amines.[51]

For instance for a series of adducts between DABCO and saturated and unsaturated dicarboxylic acids, it has been observed a high-frequency shift of about 7 ppm passing from free nitrogen to a hydrogen-bonded nitrogen N···H–O, while

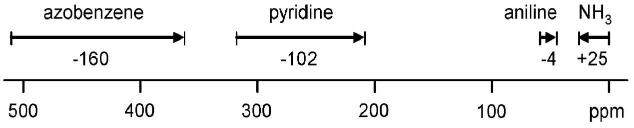

Scheme 2 Influence of hydrogen bonds on the ^{15}N chemical shift of some nitrogen-containing group.

in the case of protonated hydrogen-bonded nitrogen $^+$N–H···O$^-$ the high-frequency shift is of 20–24 ppm.[36,52]

In the case of glycine residues in solid oligopeptides, a relationship between the N···O distance and the ^{15}N chemical shift tensor in C=O···H–N HBs has been proposed.[53]

In O=C–OH···N(Py) interactions, the ^{15}N chemical shift has been used to probe the protonation state of the N atom: in moderate strength O–H···N HBs the shift is <20 ppm, in symmetric bonds O···H···N it is around δ −60, and in ionic bonds $^-$O···H–N$^+$ it becomes δ −100.[54]

In the case of evaluating the neutral or the ionic character of supramolecular complexes such as the organometallic 1,1′-dipyridylferrocene-anthranilic acid $\{[\mathrm{Fe}(\eta^5\text{-}\mathrm{C_5H_4\text{-}C_5H_4N})_2]\text{-}[(\mathrm{C_6H_4})\mathrm{NH_2COOH}]\}_2$ adduct (Fig. 8), comparing the free pyridine nitrogen chemical shift with that of the pyridine nitrogen in the adduct resulted in the confirmation of the presence of a strong O–H···N interaction with no proton transfer from the acid to the nitrogen base and of a weak N–H···N interaction.[55]

Claramunt *et al.* reported the ^{15}N CPMAS studies of six N-unsubstituted pyrazoles.[56] The ^{15}N chemical shift combined with ^{13}C CPMAS, X-ray and DFT data allowed a prediction of the tautomer and of the degree of aggregation (dimer, trimer, … motif) of the structure present in the solid state. In the case of 5-isopropyl-3-phenyl-1*H*-pyrazole it has been also possible to establish, with certainty, the tautomer and, with high probability, the tetrameric nature of this compound without knowing the X-ray structure.

Chemical shift anisotropy

HB interactions have also been studied by ^{13}C CPMAS spectroscopy.[57] Solid-state ^{13}C NMR studies of protonated and deprotonated carboxylates in amino acids have shown that the values of the principal elements of the nuclear shielding tensor change significantly with the protonation state of the carboxylic groups.[58]

The magnitudes of the principal elements of the ^{13}C CSA tensor can be measured easily from the 1D ^{13}C CPMAS spectrum obtained at a low spinning speed (*ca.* 1.5–2.0 kHz).

Isotropic ^{13}C chemical shifts linearly increase with decreasing N···O distances whereas ^{13}C chemical shift tensors of carbonyl carbon atoms of L-alanine residues in peptides, determined by spinning sideband pattern analysis, are a clear indication of the presence of a HB interaction.[57] The ^{13}C carbonyl CSA was found to correlate with the backbone hydrogen-bonding distance, especially the δ_{22} tensor element which is very sensitive to the C=O···H–N length.[59]

The orientation of the three CSA tensors for a generic carboxylic group COOH is depicted in Fig. 9.

δ_{11} lies in the plane of symmetry of the carboxylic group and it is directed along the C–C axis in the deprotonated form and perpendicularly to the C=O group in the protonated case, δ_{22} lies perpendicular to the plane of symmetry of the C=O and it is the most diagnostic parameter reflecting the strength of the HB. δ_{33}, the most shielded tensor, is perpendicular to the plane of symmetry.

The carbon chemical shift tensors of the COOH group obtained from the sideband intensity of low speed spinning NMR spectra, provide a reliable criterion for assigning the protonation state of compounds. A typical example has been reported in the case of the hydrogen-bonded supramolecular adducts between the diamine DABCO and dicarboxylic acids of variable chain length.[35] The ^{13}C CPMAS spectrum of the DABCO–glutaric acid adduct $[\mathrm{N(CH_2CH_2)_3N}]\text{–H–}[\mathrm{OOC(CH_2)_3COOH}]$ obtained at low spinning speed (Fig. 10) is indicative of the difference in the sideband pattern between the COOH (δ_{iso} 176.5) and the COO$^-$ groups (δ_{iso} 181.8 ppm).

In the $[\mathrm{N(CH_2CH_2)_3N}]\text{–H–}[\mathrm{OOC(CH_2)_{\mathit{n}}COOH}]$ (n = 1–7) adducts the chemical shift tensors, obtained by computer simulation of the spectrum measured at low spinning speed with the Herzfeld–Berger method,[60] demonstrate that δ_{11} values change from 242 ± 2 ppm (carboxylate form) to 257 ± 4 ppm (carboxylic form), δ_{22} values are of 177 ± 10 ppm for the COO$^-$ group and 155 ± 20 ppm for the COOH moiety. δ_{33} is usually not very sensitive to the protonation state of the carboxylic group, whereas δ_{iso} increases in shielding upon protonation, but unfortunately the information is limited by the fact that δ_{11} and δ_{22} change their values in opposite direction (Fig. 11).

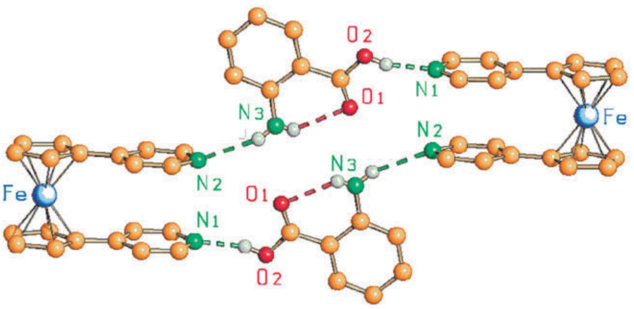

Fig. 8 X-Ray crystal structure of dipyridylferrocene-anthranilic acid. Reproduced with permission from ref. 55. Copyright 2007, RSC.

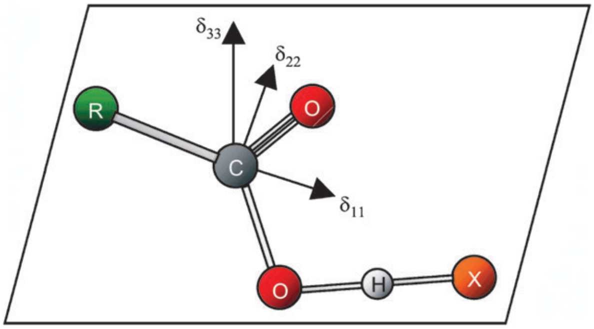

Fig. 9 Orientation of chemical shift tensors (δ_{11}, δ_{22} and δ_{33}) in carboxylic groups.

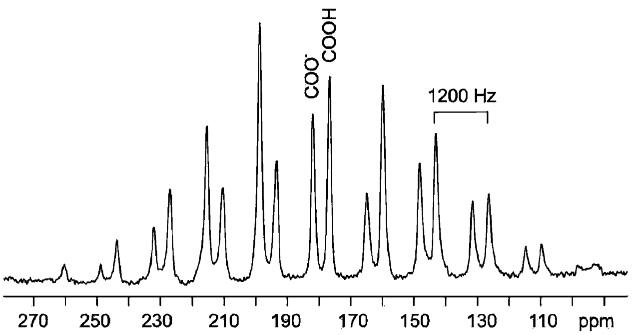

Fig. 10 Carboxylic region of the ^{13}C CPMAS spectrum of DABCO–glutaric acid adduct recorded at a spinning speed of 1.2 kHz. It shows a carboxylic and a carboxylate signal with the respective spinning sideband patterns. Reproduced with permission from ref. 35. Copyright 2003, Wiley-VCH Verlag GmgH & Co. KGaA.

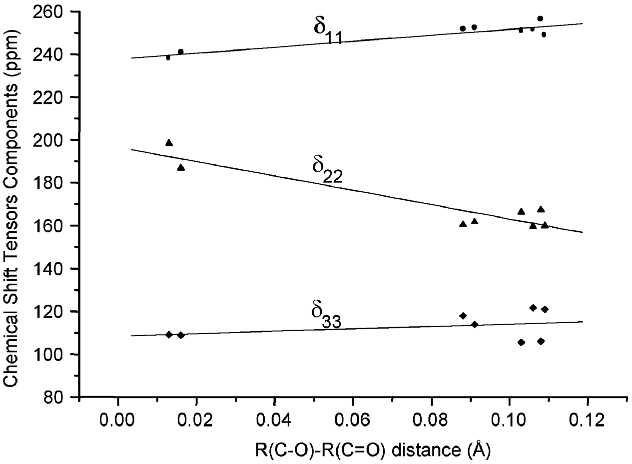

Fig. 11 Chemical shift tensor components (δ_{11}, δ_{22} and δ_{33}) of DABCO-dicarboxylic acid compounds plotted as function of the difference between the C–O and C=O bond lengths from crystallographic data. Reproduced with permission from ref. 35. Copyright 2003, Wiley-VCH Verlag GmgH & Co. KGaA.

Relaxation parameters

Spin–lattice proton relaxation times T_1 provide a versatile experimental route for evaluating molecular motion in the solid state. Indeed it is possible to investigate the dynamic behaviour of supramolecular adducts in the solid state such us rotation around bonds or reorientation. A simple way of obtaining this information is to measure the ^{1}H relaxation time at variable temperature in the wideline mode. Assuming that a single correlation time τ_c dominates the modulation of the dipolar interaction in the various temperature regimes, the T_1 values obey the Kubo–Tomita type relation:[61]

$$T_1^{-1} = C[t_c/(1 + \omega^2\tau_c^2) + 4\tau_c/(1 + 4\omega^2\tau_c^2)] \qquad (1)$$

where C is the motional constant, ω is the angular Larmor frequency, and τ_c is the correlation time of the motion expressed by the Arrhenius equation:

$$t_c = \tau_0 \exp(E_a/RT) \qquad (2)$$

τ_0 and E_a are the correlation motion in the limit of the infinite temperature and the activation energy of the motion, respectively.

We reported a T_1 relaxation analysis combined with potential energy surface (PES) calculations for a series of supramolecular adduct obtained by reacting the DABCO with saturated and unsaturated dicarboxylic acids: namely fumaric, malonic, maleic and hydromuconic [HOOC–CH$_2$–(CH)$_2$–CH$_2$–COOH] acids.[52] The optimised motional parameters calculated by the experimental T_1 data have been compared with the activation energies obtained by potential energy surface (PES) calculations. The NMR method afforded quantitative information such as the activation energy which was approximately 14–21 kJ mol^{-1} for the dynamic processes occurring in the solid state. On the other hand the PE calculations based on the structural data allowed the individuation of the rotation of the DABCO molecule along the O···H···N HBs as the probable source of relaxation for the protons in the solid adducts. Indeed the experimental activation energies were in agreement with the potential barriers associated with the reorientational process of DABCO on the basis of attractive and repulsive electrostatic interactions with atoms or nearby molecules.

Isotopic effect

Additional understanding of the HB can be gained by investigation of the hydrogen/deuterium (H/D) isotope effect. Although only a few studies on the deuterium isotope effect in the solid state have been reported[15,62] this is potentially a useful parameter for the investigation of strong HB. It has been shown by several authors,[63] that the replacement of the HB proton by a deuteron leads to a geometric isotope effect. We shall consider a generic A···H···B HB (see Scheme 3, where q_1 is the distance of the proton with respect to the HB centre and q_2 is the heavy atom distance A···B).

It has been suggested that there is a primary and a secondary geometric influence on the H/D isotope effect. The former refers to the different positions of the proton and of the deuteron with respect to the centre of the A···B interaction, *i.e.*, the q_1 value, whereas the latter refers to the change of the distance (q_2) between heavy atoms. When the hydrogen is replaced by a deuterium, the smaller heavy atom-hydrogen distance decreases, but the distance from the larger atom increases even more, leading to a widening of the HB (q_2 value increases). Such geometry changes lead also to a H/D isotope effect on the chemical shift of the neighbour atoms.

The shift experienced by the atoms involved in the interaction depends on the strength of the HB and on the position of the hydrogen atom along the heavy atom axes *i.e.* only strong HBs give an isotope effect.

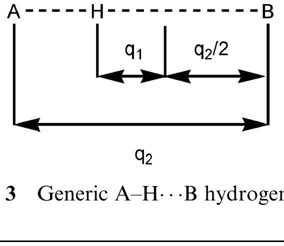

Scheme 3 Generic A–H···B hydrogen bond.

For example, the isotope effect on the ^{15}N chemical shift has been measured for a series of supramolecular adducts obtained by grinding DABCO with several deuterated dicarboxylic acids (malonic, succinic, …). As expected, no shifts on deuteration are observed in the cases of the DABCO–malonic and DABCO–glutaric adducts, characterized by weak HBs. In fact it is well-known that weak HBs do not show any H/D isotopic effect on the neighbour atom chemical shifts. Conversely, a low-frequency shift is found for the adducts with succinic, adipic, pimelic, suberic and azelaic where the deuteration decreases the O–D distance and then increases the N–D distance, confirming the formation of a LBHB for such samples.

Guest dynamics in inclusion compounds

A separate class of supramolecular systems is represented by inclusion compounds, defined as the adducts formed by the inclusion of guest molecules into cavities created by host molecules (CD molecules, zeolites, aluminosilicates, *etc*.). Host–guest adducts have been the subject of a great number of studies devoted to investigate their structure, stoichiometry and the nature of their interactions.[64] Inclusion complexes are being used as drug delivery agents[65] and chemical sensors,[66] but these molecular recognition properties can also be exploited in a way similar to an enzyme–substrate binding process.[67] Industrial processes involving enantiomeric enrichment, isomer separation and removal of undesired compounds have been tackled using inclusion complexes.[68]

Once included these compounds not only offer structural properties different from the pure compounds but they can also provide useful catalytic activities. In some cases encapsulation of a guest molecule in a host cavity allows extreme regiospecificity and stereoselectivity in the product formation.[69]

In the field of supramolecular systems CD inclusion compounds provide excellent examples of complexes formed by non-covalent intermolecular interactions.[70]

The ability of the CD hydrophobic cavity to include inorganic and organic molecules to form host–guest supramolecular adducts has been demonstrated to be dependent on the size of the internal cavity which can vary from 5 to 7 to 8 Å for α-, β- and γ-CDs, respectively (Fig. 12).

The dominant role of van der Waals interactions in the formation of host–guest complexes has been demonstrated,[71] but in some specific cases these forces are enhanced by additional hydrogen bonding arising from the CD hydroxyl groups and polar groups on the guest molecule.[59] Lower activation energy barriers are expected for the motion of molecules within the cavity or channel of a matrix due to the decrease of interatomic forces between the molecules. On the other hand it is clear that any detailed information as to any kind of dynamics which could be taking place within the cavity could enhance or hinder their applications.

Interplay of molecular size and symmetry on the dynamics of inclusion complexes

Although a large array of host–guest compounds involving CDs have been studied extensively, relatively few papers exploring guest dynamics mediated by the host–guest interactions have been reported.

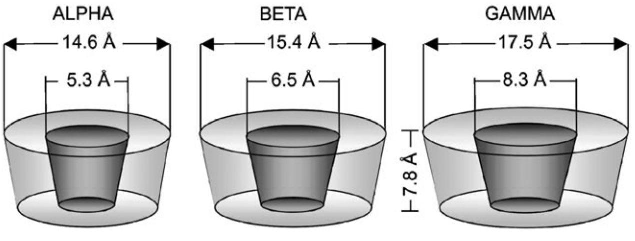

Fig. 12 Dimensions of α-, β- and γ-cyclodextrins (CDs).

As an example, an early study on included ferrocene and ruthenocene complexes within CD cavities demonstrated[72] by spin–lattice relaxation time measurements in the laboratory and rotating frames, as well as proton second moment analysis, the high mobility of the ferrocene and ruthenocene guest molecules.

Terao and coworkers[73] were able to show later, by using one-dimensional switching-angle sample spinning NMR spectroscopy, that the ferrocene molecule is precessing making an angle β of 69° with its fivefold axis in γ-CD, whereas the three different ferrocene molecules enclathrate in β-CD precess with β values of 6, 30 and 43°, respectively.

Isotropic motion in the cavity

We found several cases in which the nature of the motion of the guest molecules within the host CD cavity is dependent on the symmetry, size and resulting orientation of guest molecule within the host cavity.

Metal carbonyl complexes studied by solid-state ^{13}C NMR are shown to have altered reorientational dynamics when included in the host CD cavity compared to the parent molecular crystals.

An example is the dynamics of solid iron pentacarbonyl [$Fe(CO)_5$] which have been investigated by Hanson and coworkers in 1989.[74]

From the observation of a single carbonyl resonance at -28 °C in the ^{13}C MAS NMR the authors proposed an axial–equatorial exchange *via* a Berry pseudorotation, before the solid melts. The ^{13}C CPMAS spectrum of the ^{13}C enriched $Fe(CO)_5$/β-CD inclusion complex at a MAS rate of 5 kHz shows a single isotropic peak for the carbonyl groups with no spinning sidebands.[75] At -80 °C the ^{13}C CPMAS NMR spectrum is identical to that recorded at ambient temperature. The ^{13}C wideline spectrum of a sample ^{13}CO enriched sample of $Fe(CO)_5$ in β-CD shows a narrow peak with a bandwidth at half-height of *ca.* 20 ppm. For a carbonyl group terminally bound to a metal in a rigid lattice one should expect a linewidth of the order of 400 ppm.[76] It is likely that entire $Fe(CO)_5$ molecule is relatively free to reorient inside the CD cavity, but this motion is not sufficient to explain the presence of a unique signal in the high-resolution solid-state spectrum. In other words the two motional processes are (a) an intramolecular motional process of an axial–equatorial carbonyl exchange *via* a Berry pseudorotation mechanism[76] which would equilibrate axial and equatorial environments and also lead to extensive averaging of the CSA and (b) effective

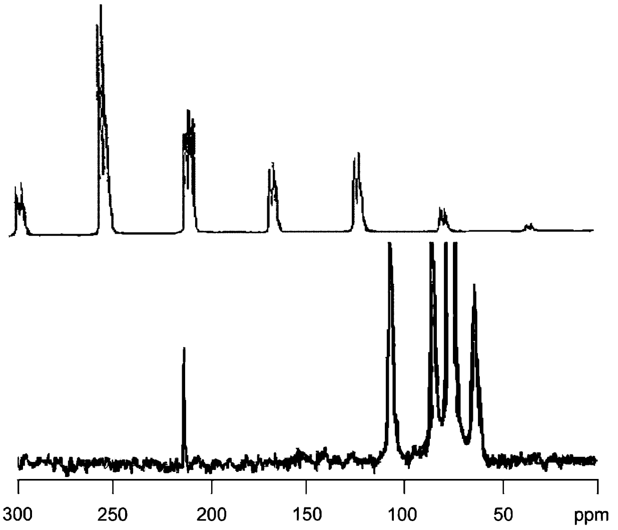

Fig. 13 Comparison between the ^{13}C CPMAS spectra of $Cr(CO)_6$ (top) and $Cr(CO)_6$ included in γ-cyclodextrin (bottom). Reproduced with permission from ref. 75. Copyright 2000, RSC.

isotropic reorientation of the whole $Fe(CO)_5$ molecule within the CD cavity which will completely average the CSA.

In the case of crystalline chromium hexacarbonyl [$Cr(CO)_6$], the comparison between the ^{13}C MAS NMR spectra of the whole molecule and its adduct with γ-CD is reported in Fig. 13. In the isotropic region of the crystalline compound four isotropic resonances are observed associated with slight distortions from octahedral crystal symmetry within the molecule.[77]

The CSA parameters associated with the spinning sideband pattern are consistent with the rigidity of the carbonyl groups in the crystal lattice. Conversely in the room temperature ^{13}C CPMAS spectrum of the γ-CD intercalation compound the presence of a single carbonyl resonance at 215.2 ppm with no spinning sidebands even at low spinning speed provides a clear evidence of a fast and isotropic reorientation of the entire $Cr(CO)_6$ molecule inside the γ-CD cavity.[75]

Motion along a principal axis

It has been previously shown that in a polycrystalline sample of $Cr(CO)_3(C_6H_6)$, the arene rotates freely along its principal coordination axis whereas the carbonyl moiety is rigid on the NMR timescale at ambient temperature.[78]

The ^{13}C CPMAS NMR spectrum of $Cr(CO)_3(C_6H_6)$ compartmentalized in the β-CD cavity (Fig. 14) shows only an isotropic peak for the carbonyl groups with no spinning sideband manifold.[79] Then the solid-state spectrum is strictly analogous to the solution spectrum, and the carbonyl moiety would seem to acquire substantial mobility able to average the large CSA associated with the rigid CO ligands. We could surmise that β-CD environment provides a lower energy pathway for the motion of the carbonyl moiety. Further proof of the motion has been obtained by recording the non-spinning spectrum of the inclusion compound that displays a bandwidth of 20 ppm, markedly narrower than the broad resonances usually found in the non-spinning metal carbonyl spectra. This observed behaviour would seem to suggest that the entire organometallic molecule is free to isotropically rotate inside the cavity. However this hypothesis was ruled out on the basis of the results obtained by measuring the powder pattern of the ^{2}H NMR solid-state spectrum of the inclusion compound containing the perdeuterated $Cr(CO)_3(C_6D_6)$ isotopomer as the guest molecule. A typical deuterium powder pattern spectrum with an inner separation between the main components of 71.0 kHz is observed at 300 K. This behaviour can be only associated with a six-site nearest-neighbour jumps of the arene ring within the β-CD cavity (C6 rotation). Then it is clear that the entire guest molecule does not rotate isotropically inside the cavity, but it is involved in a fast motion around the molecular axis of symmetry. As a consequence of such motion the shielding anisotropy, defined as $\Delta\sigma = \sigma_{33} - (\sigma_{11} + \sigma_{22})/2$ with $\sigma_{11} \leq \sigma_{22} \leq \sigma_{33}$ and $\sigma_{ii} = -\delta_{ii}$, of the axially symmetric ^{13}CO tensor is reduced according the following equation:

$$\Delta\sigma' = [(3\cos^2\beta - 1)/2]\Delta\sigma \qquad (3)$$

where β is the angle between the principal chemical shift tensor axis and the rotational axis (Scheme 4). Since in the case of $Cr(CO)_3(C_6H_6)$ the principal axis of the chemical shift for the carbonyl groups lies at an angle close to 54.7° (the "so called magic angle") the shielding anisotropy is scaled to a value close to 0.

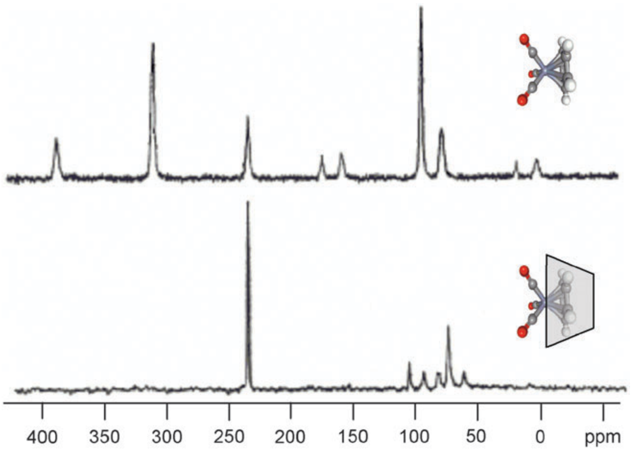

Fig. 14 Comparison between the ^{13}C CPMAS spectra of $Cr(CO)_3(C_6H_6)$ (top) and $Cr(CO)_3(C_6H_6)$ included in β-cyclodextrin (bottom). Reproduced with permission from ref. 79. Copyright 1999, RSC.

Another case is represented by $FeCp(CO)_2I$.[80] In the crystalline $FeCp(CO)_2I$ the static nature of the carbonyls is demonstrated by the presence of a large manifold of spinning sidebands associated with the isotropic resonances at 211.3 ppm. The analysis of their tensor components affords a $\Delta\sigma$ value of 411 ppm. The smaller extent of the spinning sideband pattern associated with the Cp resonance at 81.3 ppm is indicative of a fast motion of the Cp ring. This situation is characteristic of half-sandwich complexes where the fast ring rotation is allowed at most instrumentally obtainable temperatures, whereas the crystalline packing constrain does not permit the same for the carbonyl moieties.

The ^{13}C CPMAS spectrum of $FeCp(CO)_2I$ in its β-CD intercalation compound shows the appearance of small but

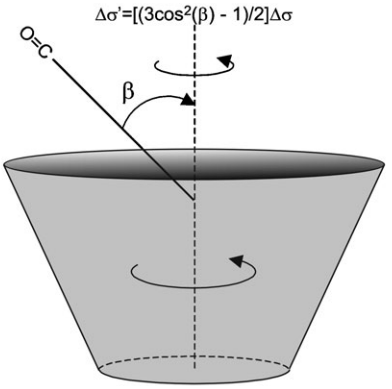

Scheme 4 Reduction of the chemical shift anisotropy ($\Delta\sigma$) of a carbonyl group.

significant spinning sideband manifold for the carbonyl resonance at 208.3 ppm only when the spinning speed is reduced to 2 kHz. A $\Delta\sigma$ value of about 60 ppm is obtained by computer simulation of the spinning sideband pattern. Since the anisotropy of mobile nuclei is reduced by a factor of $(3\cos 2\beta - 1)/2$ a β angle of about 49° has been calculated. Thus, the presence of a precessional motion of the entire molecule with respect the main symmetry Z axis of the CD cavity has been proposed, as depicted in Scheme 5. It is worth noting that such a motion has a very low energy barrier since it cannot be stopped even at the lower attainable temperature (133 K).

$FeCp(CO)_2CH_3$ represents a unique case in which the degree of motion is higher for the pure compound than for the inclusion host–guest complex. The crystalline compound displays plastic crystal-like behaviour at ambient temperature as observed from its ^{13}C CPMAS spectrum (Fig. 15, bottom). By decreasing the temperature at 263 K, the spinning sideband pattern of the individual resonances are detected and a value of 335 ppm is calculated for the $\Delta\sigma$ of the carbonyl peak (Fig. 15). When included in β-CD its room-temperature ^{13}C CPMAS spectrum recorded at low spinning speed shows two resonances in the carbonyl region with a spinning sideband pattern that allows the calculation of a $\Delta\sigma$ value of 34 ppm. By applying the eqn (3) a β angle of 51° has been estimated; then the dynamic behaviour of $FeCp(CO)_2CH_3$ in β-CD is quite similar to that found for $FeCp(CO)_2I$ discussed above.

It is evident that in this case the shape of the guest, the size of the host and the strength of the intermolecular forces do not allow an isotropic motion of the metal complex. Then only the rotation of the entire molecule along certain axis is permitted.

Motion of a part of a molecule

A particular case of mobility inside a CD cavity is represented by the $Mo_2Cp_2(CO)_6$–β-CD adduct which shows more unusual results with respect those presented above.[80]

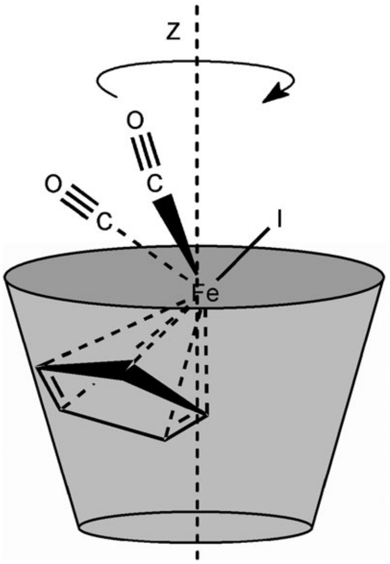

Scheme 5 Precession motion of $FeCp(CO)_2I$ in β-cyclodextrin. Reproduced with permission from ref. 80. Copyright 2007, Wiley-VCH Verlag GmgH & Co. KGaA.

At first glance the ambient temperature ^{13}C CPMAS spectrum of $Mo_2Cp_2(CO)_6$ included in γ-CD does not differ greatly from the spectrum recorded for the polycrystalline specimen. Furthermore the spinning sideband pattern associated with the carbonyl resonances looks quite similar in the two spectra. However, as shown in Fig. 16, when the temperature is decreased the overall intensity of the spinning sidebands increases with an increasing complexity of the isotropic region. Thus, different motional regimes of the two halves of $Mo_2Cp_2(CO)_6$ have been proposed. In other words the half of the moiety inside the γ-CD cavity is involved in a fast motion at RT due to the presence of weak constrains forces, whereas the non-included $MoCp(CO)_3$ moiety is rigid interacting with other $MoCp(CO)_3$ groups of neighbouring molecules in the crystalline lattice, yielding the larger contribution to the spinning sideband manifold at RT.

By decreasing the temperature, the rotation inside the cavity is slowed down and more resonances become detectable in the centre band.

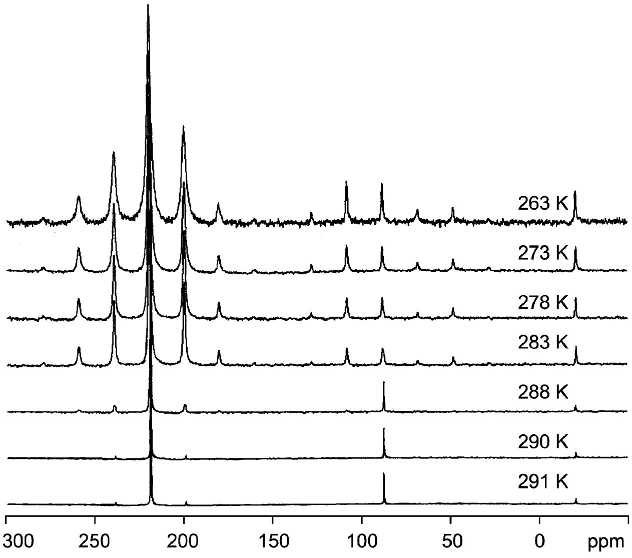

Fig. 15 Variable temperature ^{13}C CPMAS spectra of $FeCp(CO)_2CH_3$. Reproduced with permission from ref. 80. Copyright 2007, Wiley-VCH Verlag GmgH & Co. KGaA.

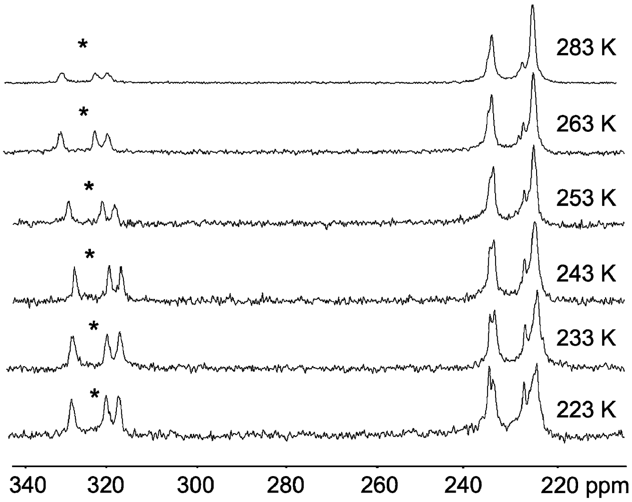

Fig. 16 Variable-temperature ^{13}C CPMAS spectra (carbonyl region) of $Mo_2Cp_2(CO)_4$ included in β-cyclodextrin. The first-order spinning sidebands are marked with an asterisk (*). Reproduced with permission from ref. 80. Copyright 2007, Wiley-VCH Verlag GmgH & Co. KGaA.

Isomer interconversion in the cavity

^{13}C CPMAS NMR studies of the structure and dynamics of the novel inclusion compound of $[Fe_2(\eta^5\text{-}C_5H_5)_2(CO)_4]$ with γ-CD represents an interesting extension of the concept of how the interplay of symmetry, size and resulting orientation of the guest molecule affects the nature of the intermolecular interactions between guest and host.[81] In this case the dynamics in a solid-state inclusion environment represents a different regime in comparison with both solution and crystalline situations. The dynamic behavior of $[Fe_2(\eta^5\text{-}C_5H_5)_2(CO)_4]$ in solution as well as in the solid state has been demonstrated by several authors.[82] The *cis* and *trans* carbonyl-bridged isomers interconvert rapidly at ambient temperature and since bridging-terminal carbonyl exchange is rapid for the *trans* isomer at all accessible temperatures, at ambient temperature a single averaged carbonyl resonance is observed. At lower temperatures the isomerization process is frozen into the limit of slow exchange and separate resonances are observed for bridging and terminal carbonyls of the *cis* isomer (Scheme 6).

High-resolution solid-state ^{13}C CPMAS spectra of ^{13}CO enriched crystalline samples of *cis* and *trans* isomers of $[Fe_2(\eta^5\text{-}C_5H_5)_2(CO)_4]$ show the expected bridging and terminal signals with a large array of spinning sidebands.[80] The intensities of the spinning sidebands analyzed by the Herzfeld–Berger method afforded the principal components of the carbonyl carbon shielding tensors that are associated with a rigid environment in the crystallographic lattice.

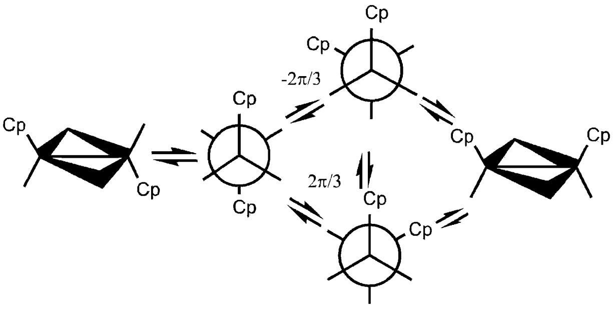

Scheme 6 *cis–trans* isomerization and carbonyl exchange in $Fe_2(\eta^5\text{–}C_5H_5)_2(CO)_4$. Reproduced with permission from ref. 82*b*. Copyright 2007, American Chemical Society.

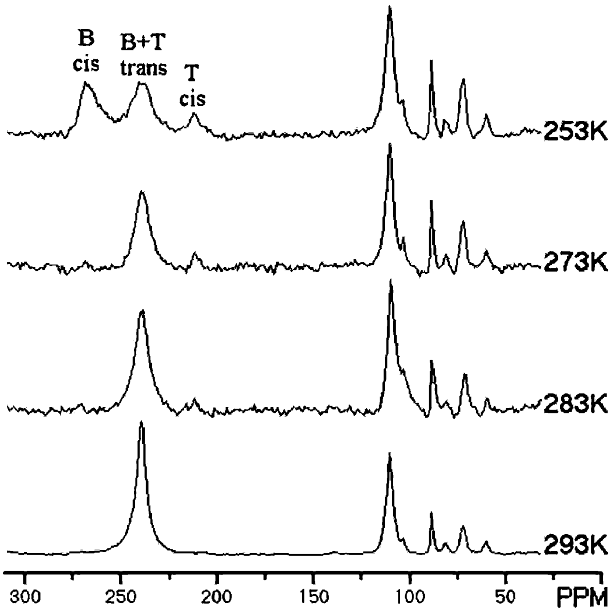

Fig. 17 Variable-temperature ^{13}C CPMAS spectra of $Fe_2(\eta^5\text{-}Cp)_2\text{-}(CO)_4$ in γ-cyclodextrin.

The single carbonyl resonance observed at 234.3 ppm in the room-temperature ^{13}C CPMAS NMR spectrum of $[Fe_2(\eta^5\text{-}C_5H_5)_2(CO)_4]$ included in γ-CD is a clear indication of a highly fluxional system. Moreover the lack of a spinning sideband pattern is a further evidence of the efficient averaging of the CSA by extensive mobility of the molecules inside the CD cavities. At lower temperature (Fig. 17) the presence of three peaks assigned to bridging, *trans* averaged and terminal environments, supports the idea that the organometallic compound included in γ-CD parallels the intramolecular fluxional processes clearly demonstrated in the solution state (Scheme 6), namely: (a) rapid terminal-bridging carbonyl exchange for the *trans* isomer at all accessible temperatures and (b) *cis–trans* isomerization. Nevertheless the environment provided to $[Fe_2(\eta^5\text{-}C_5H_5)_2(CO)_4]$ by γ-CD in the solid inclusion compound permits fluxionality, but the "host–guest" intermolecular forces appear to hinder *cis–trans* isomerization more than they do terminal–bridging carbonyl interchange.

Conclusions

We hope that we have provided enough evidences in this article to show how solid-state NMR affords valuable and detailed insight into the structure and the dynamic of a wide range of complex supramolecular architectures. This account outlined the recent progress in this field having a focus on our contributions that we have made since 2000 at the University of Torino. The use of a multinuclear and multiparametric approach in the solid-state NMR investigation allows to obtain information at the local level opening new perspectives in the prediction and design of supramolecular systems. Hydrogen bonds, polymorphism, intermolecular packing arrangements and dynamics of molecular segments can be investigated in great detail, in most cases without the need for special sample preparation.

Of particular interest is to delineate the unique role of solid-state NMR in hydrogen bond characterisation and classification. New insights has been achieved by considering: (1) the proton transfer from acids to bases evaluated by the ^{13}C CPMAS isotropic chemical shift, ^{13}C chemical shift anisotropy of carboxylic groups and by the ^{15}N CPMAS chemical shift of nitrogen atoms; (2) the strength of interactions evaluated by comparing the ^{1}H MAS chemical shift of hydrogen-bonded protons with O–O and N–O bond lengths; (3) dynamics of molecules in the crystal packing evaluated by comparing T_1 relaxation analysis and potential energy surface data; (4) the X–H distance by means of an effective method that combines ^{1}H MAS NMR and DFT calculation. This article wanted also to highlight that when weak forces are involved in a supramolecular structure there is a decrease of the energy barriers associated to the motion of groups or of entire molecules in the crystal packing.

Stereochemical non-rigidity of the carbonyl ligands in transition metal carbonyl complexes that represents a common feature in solution state is usually lost in the crystalline samples, but can be re-established, provided that the high potential energy barriers present in the crystalline framework are removed or deduced in the CD cavity.

The dynamic regime of a molecule in a inclusion environment (such for example the solid-state mobility of host–guest complexes of organometallic molecules in cyclodextrin) represents an intermediate situation between solution and crystalline state and it can be useful for understanding both dynamic regimes. This study opens new perspectives for "engineering" specific inclusion environment for molecular motion that are not accessible in solution or simple crystalline situations. This implies new possible applications in important fields such as drug delivery, sensor probes, heterogeneous catalysis. Also it is a very clear illustration of how the study of molecular dynamic behavior by solid-state NMR spectroscopy may elucidate, in a detailed fashion, aspects of the structure in materials which are not amenable to study by diffraction techniques.

Acknowledgements

We thank the Italian MURST (Prin 2006035198_004) for the financial support. We are indebted with Dario Braga, Fabrizia Grepioni, Silvio Aime and Edward Rosenberg for the helpful discussions. Most importantly we thank each and every student that was involved in the research and development of the projects described above over the past several years.

References

1 J. W. Steed and J. L. Atwood, in *Supramolecular Chemistry*, Wiley, Weinheim, 2000.
2 (*a*) C. A. Schalley, T. Weilandt, J. Bruggemann and F. Y. Vogtle, *Top. Curr. Chem.*, 2004, **248**, 141–200; (*b*) Kobuke, *Struct. Bonding*, 2006, **121**, 49–104.
3 D. K. Smith, *Chem. Commun.*, 2006, 34–44.
4 A. J. Sandee and J. N. H. Reek, *Dalton Trans.*, 2006, 3385–3391.
5 G. V. Oshovsky, D. N. Reinhoudt and W. Verboom, *Angew. Chem., Int. Ed.*, 2007, **46**, 2366–2393.
6 (*a*) D. K. Smith and F. Diederich, *Top. Curr. Chem.*, 2000, **210**, 183–227; (*b*) S. C. Zimmerman and L. J. Lawless, *Top. Curr. Chem.*, 2001, **217**, 95–120; (*c*) J. M. J. Fréchet, *Proc. Natl. Acad. Sci. USA*, 2002, **99**, 4782–4787; (*d*) F. Diederich and B. Felber, *Proc. Natl. Acad. Sci. USA*, 2002, **99**, 4778–4781; (*e*) P. J. Gittins and L. J. Twyman, *Supramol. Chem.*, 2003, **15**, 5–23.
7 (*a*) J.-M. Lehn, *Angew. Chem., Int. Ed. Engl.*, 1990, **29**, 1304; (*b*) G. R. Desiraju, in *Crystal Engineering: The Design of Organic Solids*, Elsevier, Amsterdam, 1989.
8 Several authors, in *Making Crystal by Design*, ed. D. Braga and F. Grepioni, Wiley-VCH, Weinheim, 2007.
9 K. J. D. MacKenzie and M. E. Smith, in *Multinuclear Solid-State NMR of Inorganic Materials*, ed. R. W. Cahn, Pergamon, Oxford, 2002.
10 (*a*) J. Lu, P. A. Mirau and A. E. Tonelli, *Prog. Polym. Sci.*, 2002, **27**, 357; (*b*) J. Lu, P. A. Mirau and A. E. Tonelli, *Macromolecules*, 2001, **34**, 3276; (*c*) J. Lu, P. A. Mirau, I. D. Shin, S. Nojima and A. E. Tonelli, *Macromol. Chem. Phys.*, 2002, **203**, 71; (*d*) H.-J. Schneider, F. Hacket and V. Rüdiger, *Chem. Rev.*, 1998, **98**, 1755; (*e*) J. Schmider, G. Fritsch, T. Haisch and K. Müller, *Mol. Cryst. Liq. Cryst.*, 2001, **356**, 99.
11 C. A. Fyfe, in *Solid State NMR for Chemists*, C.F.C. Press, Guelph, 1983.
12 (*a*) G. A. Jeffrey and W. Saenger, in *Hydrogen Bonding in Biological Structures*, Springer-Verlag, Berlin, 1991; (*b*) L. J. Prins, D. N. Reinhoudt and P. Timmerman, *Angew. Chem., Int. Ed.*, 2001, **40**, 2382–2426.
13 (*a*) M. C. Etter, *Acc. Chem. Res.*, 1990, **23**, 120–126; (*b*) M. J. Zaworotko, *Nature*, 1997, **386**, 220–221.
14 (*a*) G. Gilli and P. Gilli, *J. Mol. Struct.*, 2000, **552**, 1–15; (*b*) T. Steiner, *Angew. Chem., Int. Ed.*, 2002, **41**, 48–76; (*c*) G. R. Desiraju, *Acc. Chem. Res.*, 2002, **35**, 565–573; (*d*) D. Braga and F. Grepioni, *Struct. Bonding*, 2004, **111**, 1–32.
15 (*a*) A. B. Xia, J. E. Knox, M. J. Heeg, H. B. Schlegel and C. H. Winter, *Organometallics*, 2003, **22**, 4060–4069; (*b*) T. A. LeGreve and A. P. Loh, *Biophys. J.*, 2003, **84**, 498A; (*c*) L. S. Khaikin, O. E. Grikina, A. V. Golubinskii, L. V. Vilkov, E. G. Atavin, R. E. Asfin and G. S. Denisov, *Dokl. Phys. Chem.*, 2003, **390**, 158–162; (*d*) G. Buemi, *Chem. Phys.*, 2002, **282**, 181–195; (*e*) G. A. Kumar and M. A. McAllister, *J. Org. Chem.*, 1998, **63**, 6968–6972; (*f*) J. G. Chen, M. A. McAllister, J. K. Lee and K. N. Houk, *J. Org. Chem.*, 1998, **63**, 4611–4619; (*g*) M. Mehring, M. Schurmann and R. Ludwig, *Chem.–Eur. J.*, 2003, **9**, 838–849; (*h*) J. Y. J. Chen and K. J. Naidoo, *J. Phys. Chem. B*, 2003, **107**, 9558–9566.
16 L. Pauling, in *The Nature of the Chemical Bond*, Cornell University Press, Ithaca, NY, 1960.
17 P. A. Frey, *Magn. Reson. Chem.*, 2001, **39**, S190–S198.
18 (*a*) A. Ranganathan, G. U. Kulkarni and C. N. R. Rao, *J. Mol. Struct.*, 2003, **656**, 249–263; (*b*) B. Hertweck, E. Libowitzky and A. J. Schultz, *Z. Kristallogr.*, 2003, **218**, 403–412.
19 V. P. Balema, K. W. Dennis and V. K. Pecharsky, *Chem. Commun.*, 2000, 1665.
20 T. P. Shakhtshneider and V. V. Boldyrev, *Mol. Solid State*, 1999, **3**, 271.
21 (*a*) G. W. V. Cave, C. L. Raston and J. L. Scott, *Chem. Commun.*, 2001, **1**, 2159; (*b*) G. Rothenberg, A. P. Downie, C. L. Raston and J. L. Scott, *J. Am. Chem. Soc.*, 2001, **123**, 8701; (*c*) F. Toda, *CrystEngComm*, 2002, **4**, 215; (*d*) G. Kaupp, *CrystEngComm*, 2003, **5**, 117; (*e*) G. Kaupp, in *Comprehensive Supramolecular Chemistry*, ed. J. E. D. Davies, Elsevier, Oxford, 1996, vol. 8, pp. 381–423; (*f*) K. Tanaka and F. Toda, *Chem. Rev.*, 2000, **100**, 1025, and references therein.
22 D. Braga, *Chem. Commun.*, 2003, 2751.
23 (*a*) D. Braga and F. Grepioni, *Chem. Soc. Rev.*, 2000, **29**, 229; (*b*) D. Braga and F. Grepioni, *Angew. Chem., Int. Ed.*, 2004, **43**, 2–11.
24 G. A. Jeffrey, in *An Introduction to Hydrogen Bonding*, Oxford University Press, Oxford, 1997.
25 (*a*) T. Kameda and I. Ando, *J. Mol. Struct.*, 1997, **412**, 197; (*b*) S. Kuroki, N. Asakawa, S. Ando, I. Ando, A. Shojii and T. Ozaki, *J. Mol. Struct.*, 1991, **245**, 69; (*c*) K. Yamauchi, S. Kuroki, I. Ando, A. Shojii and T. Ozaki, *Chem. Phys. Lett.*, 1999, **302**, 435.

26 M. J. Duer, in *Solid-State NMR: Theory and Applications*, ed. M. J. Duer, Blackwell Science Ltd, Oxford, 2001.

27 (*a*) A. E. Aliev and K. D. M. Harris, *Struct. Bonding*, 2004, **108**, 1–53; (*b*) E. Brunner and E. Stemberg, *Prog. Nucl. Magn. Reson. Spectrosc.*, 1998, **32**, 21–57.

28 (*a*) J. Brus and J. Dybal, *Macromolecules*, 2002, **35**, 10038–10047; (*b*) J. Brus, J. Dybal, P. Sysel and R. Hobzova, *Macromolecules*, 2002, **35**, 1253–1261; (*c*) P. Lorente, I. G. Shenderovich, N. S. Golubev, G. S. Denisov, G. Buntkowsky and H.-H. Limbach, *Magn. Reson. Chem.*, 2001, **39**, S18–S29.

29 (*a*) H. Eckert, J. P. Yesinowski, L. A. Silver and E. M. Stolper, *J. Phys. Chem.*, 1988, **92**, 2055–2064; (*b*) V. Bertolasi, P. Gilli, V. Ferretti and G. Gilli, *J. Chem. Soc., Perkin Trans. 2*, 1997, 945–952; (*c*) T. K. Harris, Q. Zhao and A. S. Mildvan, *J. Mol. Struct.*, 2000, **552**, 97–109.

30 U. Sternberg and E. Brumer, *J. Magn. Reson., Ser. A*, 1994, **108**, 142.

31 (*a*) K. Yamauchi, S. Kuroki, K. Fujii and I. Ando, *Chem. Phys. Lett.*, 2000, **324**, 435; (*b*) K. Yamauchi, S. Kuroki and I. Ando, *J. Mol. Struct.*, 2002, **602**, 9.

32 (*a*) T. K. Harris, Q. Zhaoa and A. S. Mildvana, *J. Mol. Struct.*, 2000, **552**, 97–109; (*b*) A. McDermott and C. F. Ridenour, *Encyclopedia of NMR*, ed. D. M. Grant and R. K. Harris, Wiley, Chichester, 1996, p. 3820; (*c*) A. S. Mildvan, T. K. Harris and C. Abeygunawardana, *Methods Enzymol.*, 1999, 219; (*d*) B. Berglund and R. W. Vaughan, *J. Chem. Phys.*, 1980, **73**, 2037; (*e*) R. K. Harris, P. Jackson, L. H. Merwin, B. J. Say and G. Hägele, *J. Chem. Soc., Faraday Trans. 1*, 1988, **84**, 3649.

33 Th. Emmler, S. Gieschler, H.-H. Limbach and G. Buntkowsky, *J. Mol. Struct.*, 2004, **700**, 29–38.

34 I. G. Shenderovich, G. Buntkowsky, A. Schreiber, E. Gedat, S. Sharif, J. Albrecht, N. S. Golubev, G. H. Findenegg and H.-H. Limbach, *J. Phys. Chem. B*, 2003, **107**, 11924–11939.

35 D. Braga, L. Maini, G. de Sanctis, K. Rubini, F. Grepioni, M. R. Chierotti and R. Gobetto, *Chem.–Eur. J.*, 2003, **9**, 5538–5548.

36 R. Gobetto, C. Nervi, E. Valfrè, M. R. Chierotti, D. Braga, L. Maini, F. Grepioni, R. K. Harris and P. Y. Ghi, *Chem. Mater.*, 2005, **17**, 1457.

37 D. Braga, L. Maini, C. Fagnano, P. Taddei, M. R. Chierotti and R. Gobetto, *Chem.–Eur. J.*, 2007, **13**, 1222–1230.

38 R. K. Harris, P. Y. Ghi, R. B. Hammond, C. Y. Ma and K. J. Roberts, *Chem. Commun.*, 2003, 2834.

39 (*a*) H. J. Jakobsen, in *Encyclopedia of NMR*, ed. D. M. Grant and R. K. Harris, Wiley, Chichester, 1996; (*b*) A. Samoson, T. Tuherm and Z. Gan, *Solid State Nucl. Magn. Reson.*, 2001, **20**, 130.

40 (*a*) I. Schnell, S. P. Brown, H. Y. Low, H. Ishida and H. W. Spiess, *J. Am. Chem. Soc.*, 1998, **120**, 11784; (*b*) S. P. Brown, I. Schnell, J. D. Brand, K. Müllen and H. W. Spiess, *J. Am. Chem. Soc.*, 1999, **121**, 6712; (*c*) S. P. Brown, X. X. Zhu, K. Saalwächter and H. W. Spiess, *J. Am. Chem. Soc.*, 2001, **123**, 4275.

41 V. Percec, M. Glodde, T. K. Bera, Y. Miura, I. Shiyanovskaya, K. D. Singer, V. S. K. Balagurusamy, P. A. Heiney, I. Schnell, A. Rapp, H. W. Speiss, S. D. Hudson and H. Duan, *Nature*, 2002, **419**, 384.

42 S. P. Brown, I. Schnell, J. D. Brand, K. Müllen and H. W. Spiess, *J. Mol. Struct.*, 2000, **521**, 179.

43 (*a*) R. Graf, A. Heuer and H. W. Spiess, *Phys. Rev. Lett.*, 1998, **80**, 5738; (*b*) T. Dollase, R. Graf, A. Heuer and H. W. Spiess, *Macromolecules*, 2001, **34**, 298; (*c*) K. Saalwächter, *Macromol. Rapid Commun.*, 2002, **23**, 286; (*d*) R. Graf, D. E. Demco, S. Hafner and H. W. Spiess, *Solid State Nucl. Magn. Reson.*, 1998, **12**, 139; (*e*) K. Saalwächter, *Chem. Phys. Lett.*, 2002, **362**, 331.

44 (*a*) H. Geen, J. J. Titman, J. Gottwald and H. W. Spiess, *J. Magn. Reson., Ser. A*, 1995, **114**, 264; (*b*) J. Gottwald, D. E. Demco, R. Graf and H. W. Spiess, *Chem. Phys. Lett.*, 1995, **243**, 314.

45 J. Schnell and H. W. Spiess, *J. Magn. Reson.*, 2001, **151**, 153–227.

46 I. Schnell, B. Langer, S. H. M. Söntjens, R. P. Sijbesma, M. H. P. van Genderenb and H. W. Spiess, *Phys. Chem. Chem. Phys.*, 2002, **4**, 3750–3758.

47 E. Diez-Peña, I. Quijada-Garrido, J. M. Barrales-Rienda, I. Schnell and H. W. Spiess, *Macromol. Chem. Phys.*, 2004, **205**, 430–437.

48 (*a*) A. Fechtenkötter, K. Saalwächter, M. A. Harbison, K. Müllen and H. W. Spiess, *Angew. Chem., Int. Ed.*, 1999, **38**, 3039; (*b*) M. Hohwy, C. P. Jaroniec, B. Reif, C. M. Rienstra and R. G. Griffin, *J. Am. Chem. Soc.*, 2000, **122**, 3218; (*c*) D. McElheny, E. DeVita and L. Frydman, *J. Magn. Reson.*, 2000, **143**, 321; (*d*) B.-J. van Rossum, C. P. de Groot, V. Ladizhansky, S. Vega and H. J. M. de Groot, *J. Am. Chem. Soc.*, 2000, **122**, 3465.

49 (*a*) R. O. Duthaler and J. D. Roberts, *J. Magn. Reson.*, 1979, **34**, 129; (*b*) R. E. Botto and J. D. Roberts, *J. Org. Chem.*, 1977, **42**, 2247.

50 C. Foces-Foces, A. Echevarria, N. Jagerovic, I. Alkorta, J. Elguero, U. Langer, O. Klein, M. Minguet-Bonvehi and H.-H. Limbach, *J. Am. Chem. Soc.*, 2001, **123**, 7898–7906.

51 G. C. Levy and R. L. Lichter, in *Nitrogen-15 Nuclear Magnetic Resonance Spectroscopy*, John Wiley & Sons, New York, 1979.

52 R. Gobetto, C. Nervi, M.R. Chierotti, D. Braga, L. Maini, F. Grepioni, R. K. Harris and P. Hodgkinson, *Chem.–Eur. J.*, 2005, **11**, 7461.

53 A. Fukutani, A. Naito, S. Tuzi and H. Saito, *J. Mol. Struct.*, 2002, **602**, 491.

54 S. N. Smirnov, N. S. Golubev, G. S. Denisov, H. Benedict, P. Schah-Mohammedi and H.-H. Limbach, *J. Am. Chem. Soc.*, 1996, **118**, 4094–4101.

55 D. Braga, S. L. Giaffreda, K. Rubini, F. Grepioni, M. R. Chierotti and R. Gobetto, *CrystEngComm*, 2007, **9**, 39–45.

56 R. M. Claramunt, P. Cornago, V. Torres, E. Pinilla, M. R. Torres, A. Samat, V. Lokshin, M. Vales and J. Elguero, *J. Org. Chem.*, 2006, **71**, 6881–6891.

57 (*a*) Z. T. Gu and A. Mcdermott, *J. Am. Chem. Soc.*, 1993, **115**, 4282–4285; (*b*) Z. T. Gu, R. Zambrano and A. Mcdermott, *J. Am. Chem. Soc.*, 1994, **116**, 6368–6372; (*c*) J. C. Facelli, Z. T. Gu and A. Mcdermott, *Mol. Phys.*, 1995, **86**, 865–872; (*d*) F. Aguilar Parrilla, G. Scherer, H.-H. Limbach, M. D. C. Foces-Foces, F. H. Cano, J. A. S. Smith, C. Toiron and J. Elguero, *J. Am. Chem. Soc.*, 1992, **114**, 9657–9659; (*e*) F. Aguilar Parrilla, H.-H. Limbach, J. Elguero, M. D. C. Foces-Foces, G. Scherer, F. H. Cano, J. A. S. Smith, C. Toiron, B. Wehrle, A. Baldy, M. Pierrot, M. M. T. Khurshid and J. B. Larcombe-McDouall, *J. Am. Chem. Soc.*, 1989, **111**, 7304; (*f*) F. Aguilar Parrilla, R. M. Claramunt, C. Lopez, D. Sanz, H.-H. Limbach and J. Elguero, *J. Phys. Chem.*, 1994, **98**, 8752–8760.

58 (*a*) Z. Gu and A. McDermott, *J. Am. Chem. Soc.*, 1995, **115**, 4262; (*b*) A. Naito, S. Ganapathy, K. Aakasaka and C. J. McDowell, *J. Chem. Phys.*, 1981, **74**, 3198; (*c*) R. Haberkom, R. Stark, H. van Willigen and R. Griffin, *J. Am. Chem. Soc.*, 1981, **103**, 2534; (*d*) N. James, S. Ganapathy and E. Oldfield, *J. Magn. Reson.*, 1983, **54**, 111; (*e*) R. Griffin, A. Pines, S. Pausak and J. Waugh, *J. Phys. Chem.*, 1975, **65**, 1267; (*f*) W. Veeman, *Prog. NMR Spectrosc.*, 1984, **16**, 193.

59 Y. Wei, D.-K. Lee and A. Ramamoorthy, *J. Am. Chem. Soc.*, 2001, **123**, 6118–6126.

60 J. Herzfeld and A. E. Berger, *Chem. Phys.*, 1980, **73**, 6021.

61 R. Kubo and K. Tomita, *J. Phys. Soc. Jpn.*, 1954, **9**, 888–919.

62 (*a*) H. Benedict, H. H. Limbach, M. Wehlan, W. P. Fehlhammer, N. S. Golubev and R. Janoschek, *J. Am. Chem. Soc.*, 1998, **120**, 2939–2950; (*b*) H. Benedict, C. Hoelger, F. AguilarParrilla, W. P. Fehlhammer, M. Wehlan, R. Janoschek and H. H. Limbach, *J. Mol. Struct.*, 1996, **378**, 11–16; (*c*) T. Dziembowska, K. Ambroziak, Z. Rozwadowski, W. Schiff and B. Kamienski, *Magn. Reson. Chem.*, 2003, **41**, 135–138; (*d*) C. M. Lagier, D. C. Apperley, U. Scheler, A. C. Olivieri and R. K. Harris, *J. Chem. Soc., Faraday Trans.*, 1996, **92**, 5047–5050.

63 (*a*) A. R. Ubbelohde and K. G. Gallagher, *Acta Crystallogr.*, 1955, **8**, 71; (*b*) A. C. Legon and D. J. Millen, *Chem. Phys. Lett.*, 1988, **147**, 484.

64 (*a*) D. D. MacNicol, J. J. McKendrick and D. R. Wilson, *Chem. Soc. Rev.*, 1978, **7**, 65–87; (*b*) J. E. D. Davies, W. Kemula, H. M. Powell and N. O. Smith, *J. Inclusion Phenom.*, 1983, **1**, 33–44; (*c*) in Crystallography of Supramolecular Compounds, , *NATO ASI Ser., Ser. C: Math. Phys. Sci.*, ed. G. Tsoucaris, J. L. Atwood and J. Lipkowski, Kluwer Academic Publishers, Dordrecht, 1996, **480**, ISBN 0-7923-4051-5; (*d*) Yu. A. Dyadin and I. S. Terekhova, in *Encyclopedia of Supramolecular Chemistry*, ed. J. L. Atwood and J. W. Steed, Marcel Dekker, New York, 2004, pp. 253–260.

65 (*a*) A. T. Florence and P. U. Jani, *Drug Safety*, 1994, **10**, 233; (*b*) T. Loftsson and M. Masson, *Int. J. Pharm.*, 2001, **225**, 15; (*c*)

B. J. Ravoo, *J. Controlled Release*, 2001, **72**, 54; (*d*) K. Uekama, F. Hirayama and T. Irie, *Chem. Rev.*, 1998, **98**, 2035.

66 (*a*) P. Shahgaldian and U. Pieles, *Sensors*, 2006, **6**, 593–615; (*b*) D. Beck, J. Brewer, J. Lee, D. McGraw, B. A. DeGraff and J. N. Demas, *Coord. Chem. Rev.*, 2007, **251**, 546–553.

67 R. S. Wylie and D. H. MacCarteney, *Inorg. Chem.*, 1993, **32**, 1830.

68 (*a*) J. Szejtli, *Pure Appl. Chem.*, 2004, **76**, 1825–1845; (*b*) E. M. M. Del Valle, *Proc. Biochem.*, 2004, **39**, 1033–1046.

69 M. D. Johnson and J. G. Bernard, *Chem. Commun.*, 1996, 185.

70 J. Szejtli, *Chem. Rev.*, 1998, **98**, 1743.

71 (*a*) E. Alvira, *Chem. Phys. Lett.*, 2007, **439**, 252–257; (*b*) S. Chelli, M. Majdoub, M. Jouini, S. Aeiyach, F. Maurel, K. I. Chane-Ching and P. C. Lacaze, *J. Phys. Org. Chem.*, 2007, **20**, 30–43.

72 Z. Narankiewicz, A. L. Blumenfeld, V. I. Bondareva, I. A. Mamediarova, M. N. Nefedova and V. I. Sokolov, *J. Inclusion Phenom. Mol. Recognit. Chem.*, 1991, **11**, 233–245.

73 F. Imashiro, D. Kuwawara, N. Kitazaki and T. Terao, *Magn. Reson. Chem.*, 1992, **30**, 796–797.

74 B. E. Hanson and K. H. Whitmire, *J. Am. Chem. Soc.*, 1990, **112**, 974.

75 H. C. Canuto, S. J. Heyes, S. Aime, R. Gobetto and F. Napolitano, *J. Chem. Soc., Dalton Trans.*, 2000, 4075–4077.

76 J. W. Gleeson and R. V. Vaughan, *J. Chem. Phys.*, 1983, **78**, 5384–5392.

77 J. H. Walter, L. Reven and E. Oldfield, *J. Phys. Chem.*, 1989, **93**, 1320.

78 (*a*) P. Delise, G. Allegra, E. R. Mognaschi and A. Chierico, *J. Chem. Soc., Faraday Trans. 2*, 1975, **71**, 207; (*b*) G. W. Wagner and B. Hanson, *Inorg. Chem.*, 1987, **26**, 2019; (*c*) S. Aime, D. Braga, R. Gobetto, F. Grepioni and A. Orlandi, *Inorg. Chem.*, 1991, **30**, 951.

79 S. Aime, H. C. Canuto, R. Gobetto and F. Napolitano, *Chem. Commun.*, 1999, 281–282.

80 S. Aime, M. R. Chierotti, R. Gobetto, A. Masic, F. Napolitano, H. C. Canuto and S. J. Heyes, *Eur. J. Inorg. Chem.*, 2008, 152–157.

81 H. C. Canuto, A. Masic, N. H. Rees, S. J. Heyes, R. Gobetto and S. Aime, *Organometallics*, 2006, **25**, 2248–2252.

82 (*a*) R. D. Adams and F. A. Cotton, *J. Am. Chem. Soc.*, 1973, **95**, 6589–6594; (*b*) D. Braga, M. R. Chierotti, N. Garino, R. Gobetto, F. Grepioni, M. Polito and A. Viale, *Organometallics*, 2007, **26**, 2266–2271; (*c*) E. Rosenberg, D. C. Harris and J. D. Roberts, *J. Chem. Soc., Dalton Trans.*, 1974, 2398; (*d*) L. J. Farrugia and L. Mustoc, *Organometallics*, 1992, **11**, 2941–2944; (*e*) L. J. Farrugia, *J. Chem. Soc., Dalton Trans.*, 1997, 1785.